A Study of Cancerous Tumors using Phase Transition Methods

Mohammad Sahrapour

December 12, 2005

Abstract

Cancer is a disease that has affected almost everyone directly or indirectly, yet we still have no effective means of predicting or controlling it. In this paper we discuss the application of two methods of physics to the problem of tumor growth. The first is a local interaction model that through many iterations generates macroscopic tumors that mimic real life tumors. This model works solely based off the interaction between neighboring cells as well as the level of nutrients available to each cell and is thus very flexible. The second model of tumor growth that we consider is that of a universal scaling law that is shown to be applicable to a wide range of organisms.

I. Introduction

In the last hundred years science has made remarkable progress on the eradication of many diseases. So much so that today many people are not aware of diseases that previously were fatal; diseases such as polio, small pox, measles, ... etc. Despite this, there exist today many illnesses that still elude a cure. One of the most deadly of these is cancer. After decades of research, today we have many effective treatment options that, when the cancer is caught in an early enough stage, many lead to a regression of the cancer and a relatively normal life for the patient. However we still cannot deterministically stop the progression of cancer. A proper understanding of the growth and spreading mechanisms of tumors may one day lead to more effective treatment options.

The term cancer refers to a wide class of diseases all with different properties, effecting different parts of the body; nevertheless they all show a similar pattern of explosive growth. As the applications of mathematical models become more prevalent in biology, a natural area for the application of these techniques is to understanding the growth of malignant tumors. To this effect many models, both analytical and numerical, have been proposed. The book by Adam and Bellomo[1] provides a good survey of the analytical techniques that have been applied to the problem. But these models, while useful for describing the initial stages of tumor growth, or growth in uniform and/or controlled environments, cannot describe tumor growth in real environments. Recently, some groups have started to apply techniques commonly used in the study of complex systems to the problem of tumor growth. In this paper we will discuss two of these approaches.

In the first part of this paper we will discuss a numerical model based on local interactions between cancer cells and their environment that is able to reproduce the major phases that are observed for cancerous tumors; namely, Unlimited growth, spread to other parts of the body (metastasis), latency, and regression. In the second part, we will describe analytical work showing power law scaling between scaled tumor mass and scaled tumor growth times. This "universal" law is shown to be valid for many kinds of tumors, from those grown in vitro in the laboratory, to in vivo tumor in humans as well as in rodents.

II. Investigation of tumor phases using a discrete model

In this section we review numerical work simulating the growth of tumors as a function of the availability of nutrients in a uniform density environment[2,3], as well as in the presence on anatomical barriers modeled as variations in the density of the environment[4]. We start with the basic model and the motivations behind it and then move on to show how the model predicts various phases for tumors. We then discuss an extension of this model to include barriers and compare the results of simulations with clinical observations of cancer in the larynx and the jaw.

A. Basic Model

The model they consider is a 2-dimensional model representing a slab of tissue, discretized on a rectangular grid. At each node of the grid they define a local population of healthy cells, $h(\vec{i})$, cancerous cells, $c(\vec{i})$, and dead cells $d(\vec{i})$ as well as the local concentration of free nutrients, $p(\vec{i})$

(assuming that all the relevant nutrients can be accounted for by a single variable p). The cell populations are normalized to one so that: $h(\vec{i})+c(\vec{i})+d(\vec{i})=1$.
An initial cancerous cell is placed at the center of the grid and the system evolves as follows:

1. The nutrients are supplied by blood vessels along the right and left edges of the grid. This is modeled by a fixed nutrient concentration p_o in nodes at the left and right boundaries. Nutrients diffuse to neighboring nodes at a constant rate of α.
2. We assume that healthy cells are static (do not move from node to node) and absorb the free nutrients at a constant, both in time and space, rate γ_h.
3. Cancerous cells _absorb_ free nutrients, p($\vec{i}$), and transform them into bound nutrients, q($\vec{i}$) at a rate of $\gamma(\vec{i})=\gamma^{as}\{1-\exp[-\Gamma\,p(\vec{i})]\}$. Here γ^{as} is the asymptotic absorption rate and Γ is the nutrient affinity parameter proportional to the number of receptors each cell has for the nutrient.
4. Cancerous cells _consume_ bound nutrients at a rate $\beta(\vec{i})=\beta^{as}\{1-\exp[-q(\vec{i})/c(\vec{i})]\}$, to maintain metabolic activity. B^{as} is the asymptotic conversion rate.
5. When the amount of bound nutrient per cell, q($\vec{i}$) / c($\vec{i}$), falls below some threshold value Q_D, a random number, r($\vec{i}$) < c($\vec{i}$), of cancerous cells in node $\vec{i}$ _die_; thereby increasing d($\vec{i}$) by r($\vec{i}$).
6. When q($\vec{i}$) / c($\vec{i}$) exceeds some threshold value Q_M , a random number, r'($\vec{i}$) < h($\vec{i}$), of cancerous cells replace healthy cells in node $\vec{i}$. In this way cancerous cells _reproduce_.
7. When q($\vec{i}$) / c($\vec{i}$) is below a threshold P_D, with $Q_D < P_D < Q_M$, then a ratio, χ, of cells _migrate_ to neighboring nodes replacing healthy cells there; if there aren't enough healthy cells to accommodate this migration, then nothing happens.
8. Finally, we count cancerous cells that migrate to the blood vessels and assume that they will contribute to _metastasis_, the spread of a tumor to previously uninfected parts of the body.

The above rules are be implemented by the following iteration equations:

First we update c($\vec{i}$) and d($\vec{i}$) for the current time step:

$$c(\vec{i},t)\rightarrow c(\vec{i},t)\{1-r(\vec{i})\Theta[Q_D c(\vec{i})-q(\vec{i})]+r'(\vec{i})\Theta[q(\vec{i})-c(\vec{i})Q_M]\}$$

Here the 2nd term corresponds to cell death and the 3rd term corresponds to reproduction (mitosis). Θ is the Heaviside step function.

$$d(\vec{i},t)\rightarrow d(\vec{i},t)+c(\vec{i})r(\vec{i})\Theta[Q_D c(\vec{i})-q(\vec{i})]$$

We then advance to the next time step:

$$c(\vec{i},t+\tau)=c(\vec{i},t)+\tau[h(\vec{i})\sum_{i'}^{NN}\alpha_1(\vec{i'})c(\vec{i'})-\alpha_1(\vec{i})c(\vec{i})\sum_{i'}^{NN}h(\vec{i'})]$$

where $\alpha_1(\vec{i})=\chi\Theta[c(\vec{i})P_D-p(\vec{i})]$ and the sum is over the nearest neighbors.

$$d(\vec{i},t+\tau)=d(\vec{i},t)$$

$$h(\vec{i},t+\tau)=1-c(\vec{i},t+\tau)-d(\vec{i},t+\tau)$$

$$p(\vec{i},t+\tau)=p(\vec{i},t)+\tau[\alpha\sum_{\vec{i}'}^{NN}[p(\vec{i}')-p(\vec{i})]-\gamma_h\,p(\vec{i})h(\vec{i})-\gamma(\vec{i})c(\vec{i})]$$

The 1st term above corresponds to diffusion of nutrients in and out of the node. The 2nd and 3rd terms correspond to nutrient consumption by healthy and cancerous cells respectively.

$$q(\vec{i},t+\tau)=q(\vec{i},t)+\tau[\gamma(\vec{i})c(\vec{i})-\beta(\vec{i})c(\vec{i})+h(\vec{i})\sum_{\vec{i}'}^{NN}\alpha_1(\vec{i}')q(\vec{i}')-\alpha_1(\vec{i})q(\vec{i})\sum_{\vec{i}'}^{NN}h(\vec{i}')]$$

The γ-term represents free to bound nutrient conversion. The β-term corresponds to the bound nutrient consumption. The last two terms are related to the bound nutrient transported by migrating cancer cells.

B. Results

Simulations were done according to the above methods on a 300 x 300 grid point lattice keeping all parameters fixed except for γ^{as} and p_o. By appropriately varying these two parameters, four types of tumors (phases) were observed. Four examples of the observed behavior can be seen in Appendix 1.

In figure 1 we see plotted cancer volume vs time for various values of γ^{as} while keeping p_o constant at 0.03. For very low values of γ^{as}, the tumor grows to some small volume, and then regresses. For slightly higher γ^{as}, we observe latency, where the tumor levels off at some fixed volume and neither grows nor shrinks. If we now slowly increase γ^{as} we reach a critical value, in this case approximately 0.075, above which there is explosive growth of the tumor; here we can see a phase transition from the latent phase to the malignant phase.

The authors then perform extensive simulations to map out a significant portion of phase space such that all 4 phases are clearly visible. The phase diagram is reproduced in figure 2. One thing to note is that as the authors themselves admit, the boundary between the metastasis and unlimited growth phases is at best representative. They arbitrarily choose a threshold Ξ and label all cases in which more than Ξ cells make it into the bloodstream before the tumor reaches a deadly size (again arbitrarily determined),
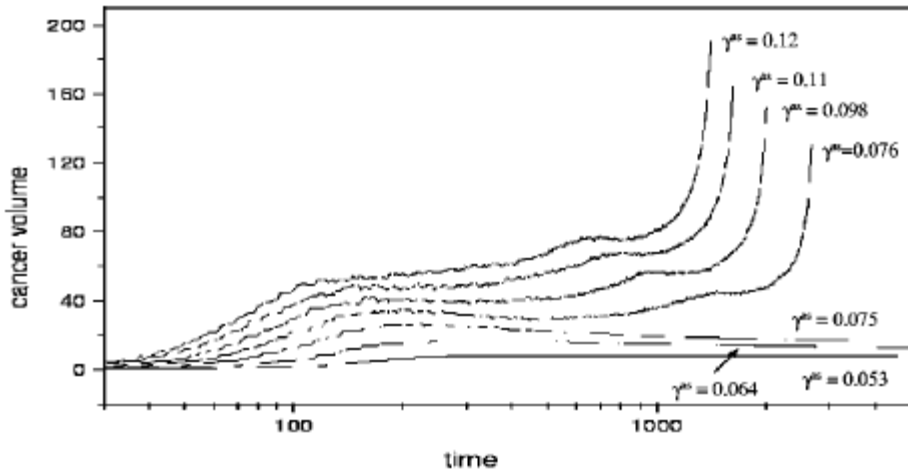

Fig. 1. Tumor growth as a function of time for different values of γ^{as}. [Delsanto et al. (2000)]

as metastasis. Despite this, it is quite impressive to see such a simple model give rise to such dynamic behavior. As the authors point out, the phase diagram suggests how sensitive tumors are to their surroundings. A very small change in p_o the availability of nutrients in the surroundings can quickly lead a tumor out of latency and bring it into a regime of rapid growth or vice versa. This perhaps could be the basis of an effective strategy against cancer.
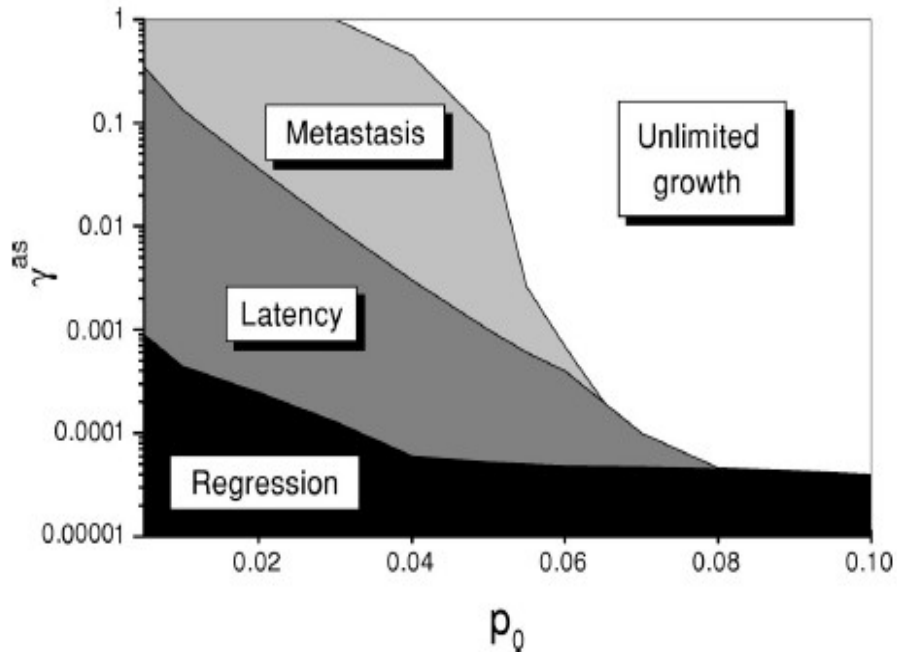

Fig. 2. Tumor phase diagram in nutrient availability vs. consumption rate space. [Delsanto et al. (2000)]

C. Extension to Anatomical Constraints

The above work, although very interesting and suggestive, fails to make any predictions and cannot easily be compared with experiments or against clinical data. The methods are probably correct but in order to advance to the next level a comparison with clinical data is necessary. Along these lines, Sansone et al.[4] have applied the model to the specific case of cancers of the larynx and oral cavity. In order to do so they needed to extend the model to include non-uniform diffusion of nutrients and cancer cells so as to model the presence of different kinds of tissue such as cartilage, muscle, and bone. The formalism is identical to the above except that now α and χ depend on the starting and ending node. Reference 4 shows some of the modified iteration equations; here we only review the results.

Figure 3 shows a comparison of two simulations and two clinical CT scans. The top row shows the CT scans, the middle row shows the simulation results using the extended methodology, and the bottom row show the results of a simulation without anatomical constraints, i.e. in a uniform tissue. The first column shows a less aggressive tumor while the second column shows a much more aggressive tumor that eventually breaks through the thyroid cartilage as can be seen in the simulation.

In the CT scans the tumor is outlines by the dotted lines while in the simulations the tumor is indicated by the light areas. The cartilage however is white in the CT scan and dark in the simulation. As can be seen, the simulation results agree at least qualitatively, both in shape and size, with the CT scans.
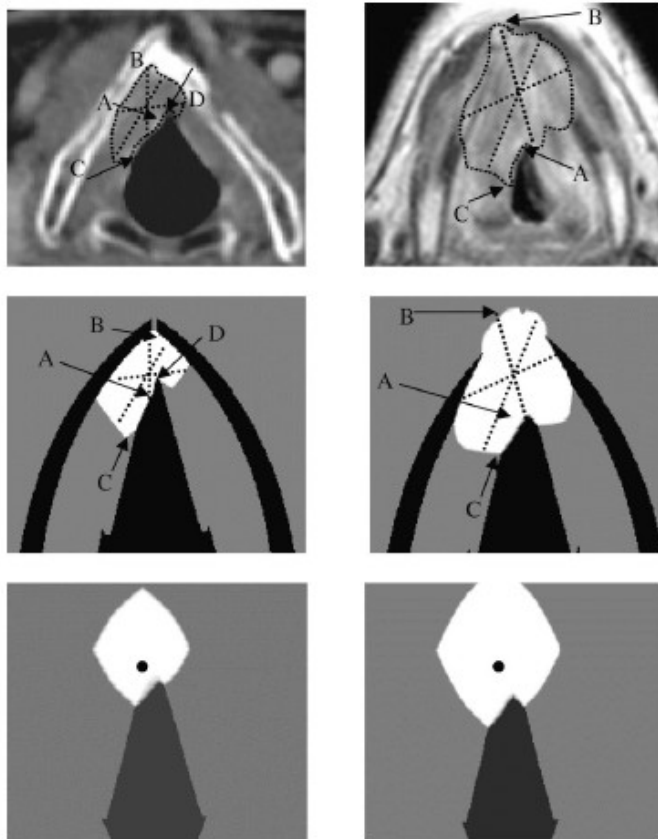
4

Fig. 4. Simulation of a tumor near the jaw bone at three different times compared with a CT scan of the same. [Sansone et al. (2001)]

Fig. 3. From top to bottom, comparison of CT scans of actual tumors. the results of simulations taking into account anatomical barriers and the results of simulations done with no barriers.[Sansone et al. (2001)]
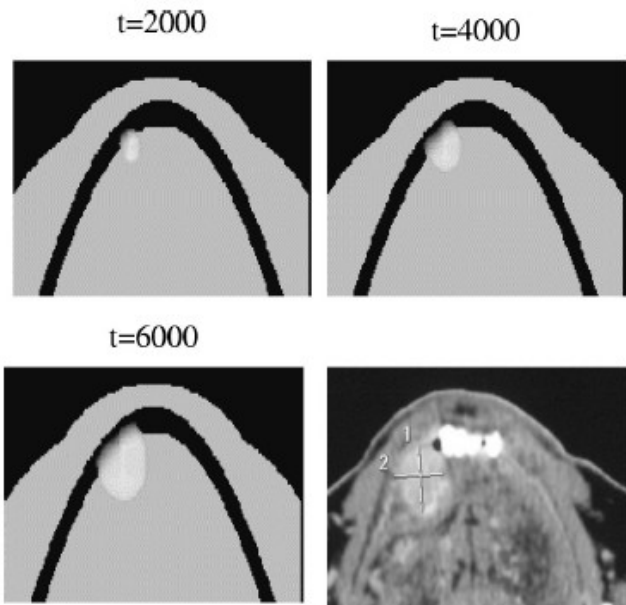
It is interesting to note the difference between the bottom two rows in figure 3. The tumors in the bottom row have a much more uniform shape and expand almost isotropically from the black dot where the tumor seed was initially placed. The tumors in the middle row however, despite having started from the same seed as those in the bottom row, show a high degree of non-uniformity. This is a good sign that the cancer is acting as we expect in the simulation, in that it is expanding much more into the soft tissue and only later, and much slower, does it start to penetrate the much harder cartilage. In this case the tumor cannot reproduce as much because of the pressure exerted by the barriers and must rely much more on diffusion to spread. In the bottom pictures however, there is no such pressure and the tumor replicates freely, leading to a much larger tumor.

To further test their model the authors simulate tumor growth in the jaw and again compare their results with a CT scan of an actual jaw tumor. The results of this simulation can be seen in figure 4. The figure shows three snapshots of the simulation at different times. As well as the CT scan. In the simulations, the jaw bone is the dark parabola whereas in the CT scan, it's only slightly darker than the rest of the tissue. The bright white spot in the CT scan is a spurious effect due to the presence of teeth. Once again the tumor is indicated by bright regions in the simulations; in the CT scan, the tumor is indicated by the cross. As before, the final simulation snapshot agrees well qualitatively with the CT scan. Interestingly even though the majority of the volume of the tumor is in the soft tissue as expected, the tumor is aggressive enough to attack and break into the bone.

This simulation method seems to show promise to accurately predict the shape and size of tumors in diverse environments and would be a good basis for further investigations. However, despite the good qualitative agreement between the CT scans and simulations, there need to be more tests done, preferably quantitative ones, to confirm it's validity.

III. A Universal Scaling Law for Growth

In this section we will review some work[5,6,7] suggesting that tumor growth follows a universal scaling law relating a scaled mass to scaled time. The basis of this work is a very interesting paper by West et al.[8] in which a universal growth law is derived and is shown to work for a wide variety of organisms. We'll first take a look at West's ideas and then move onto their application to tumors.

A. West's Model for Ontogenetic Growth

West's argument starts with a statement of the conservation of energy,

$$B = \sum_c [N_c B_c + E_c \frac{dN_c}{dt}].$$

B is the resting metabolic rate, or the total incoming energy; N_c is the total number of cells that make up the organism; B_c is the metabolic rate of a single cell; E_c is the energy needed to create a new cell; and finally the sum runs over all types of cells. The first term on the right is therefore the energy needed to maintain the organism, while the second term is the energy needed for growth. Defining m_c as the mass of one cell, we have total body mass $m = m_c N_c$, and the above equation can be rewritten as:

$$\frac{dm}{dt} = (\frac{m_c}{E_c}) B - (\frac{B_c}{E_c}) m.$$

Now West et al. assume that $B = B_o m^{3/4}$, where B_o is a constant for a given taxon (there exists some debate about the value of the exponent[9] with some who claim it is closer to 2/3; we will however continue assuming the ¾ value), then

$$\frac{dm}{dt} = am^{3/4} - bm \quad \text{with} \quad a \equiv B_o \frac{m_c}{E_c} \quad \text{and} \quad b \equiv \frac{B_c}{E_c}.$$

When dm/dt =0, the organism has reached it's maximum mass $M = (a/b)^4 = (B_o m_c/B_c)$. So we can rewrite the previous equation as

$$\frac{dm}{dt} = am^{3/4}[1 - (\frac{m}{M})^{1/4}].$$

Integrating this equation we get

$$(\frac{m}{M})^{1/4} = 1 - [1 - (\frac{m_o}{M})^{1/4}] e^{-a \frac{t}{4M^{1/4}}}$$

From this equation we see that if we plot the dimensionless mass ratio $r \equiv (\frac{m}{M})^{1/4}$ versus dimensionless time $\tau \equiv \frac{at}{4M^{1/4}} - \ln[1 - (\frac{m_o}{M})^{1/4}]$ then "all species, regardless of taxon, cellular metabolic rate (B_c), or mature body size (M), should fall on the same parameterless universal curve $r = 1 - e^{(-\tau)}$ "[8]. Figure 5 is from West et al. and shows their testing of the scaling law on many vastly different animals. As can be seen, the scaling law is a very good one.

In this formalism, r can be thought of the ratio of metabolic energy available for the maintenance of the organism, in which case we define R = 1- r to be the ratio of metabolic energy available for growth.

West notes that the reason behind this scaling law may be the fundamental imbalance between the fractal-like network of capillaries that supply the organism which scale as $m^{3/4}$ and the number of cells

6

needing nourishment which scales as m. This imbalance eventually leads to a slowing down and ultimately a halt in the growth of the organism.
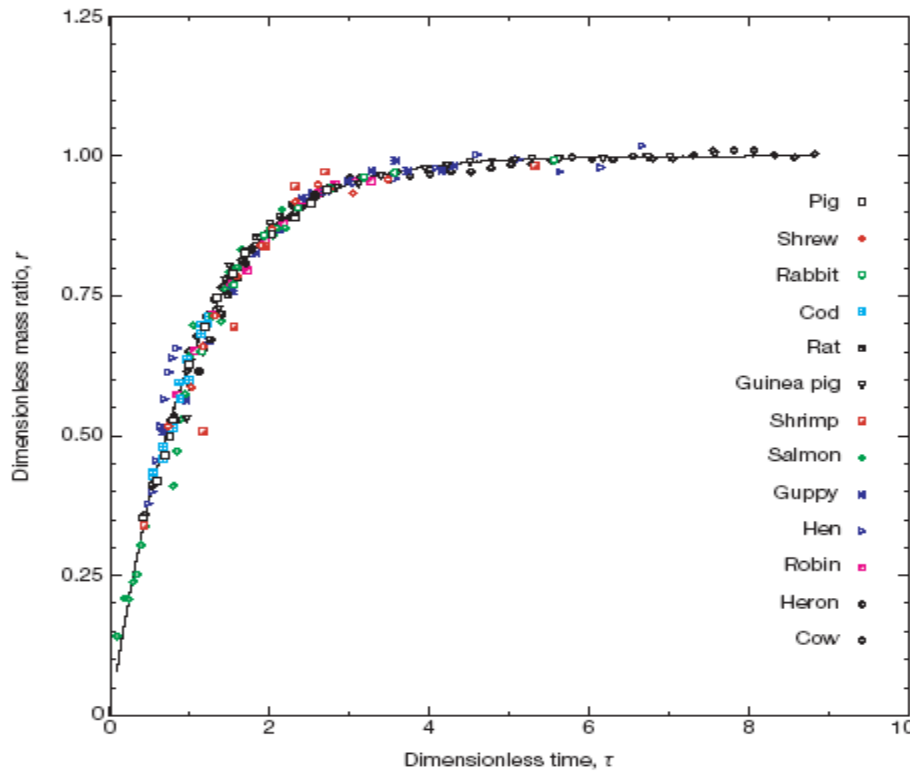

Fig. 5. Mass ratio vs. dimensionless time. When plotted this way West et al. predict all data should fall on the same curve $1 - e^{-\tau}$, shown as a solid line. *[West et al. (2001)]*

B. Scaling Law for Tumor Growth

We will now discuss an application of West et al.'s scaling law to tumors as undertaken by Guiot et al.[5] In the case on a tumor, m_0 and M correspond respectively to the initial and final masses of the tumor. For a given dataset(tumor mass versus time) Guiot et al. started by using the smallest and largest values of m as m_o and M respectively. This gives a first estimate of the parameter a as defined above. They then used this estimate for a, and varied m_o and M to find a better fit to the data. Using these new values of m_o and M, they reestimate a and repeat the process until the best fit to the biological data is obtained.

In Appendix 2 we reproduce plots of rescaled tumor mass versus rescaled time from Guiot's paper. The solid line on each graph represents West's uniform scaling law. Just as with the animal data, the scaling law seems to fit the tumor data very well.

Perhaps the reason the tumor data fits the scaling law so well is that like all other organisms, the basic governing rule is that of supply and demand. The same arguments as above apply here, the supply of nutrients cannot keep up with the explosive growth of the tumor and so the tumor reaches a maximum size. At this point the tumor must diffuse to other regions in order to continue growing.

It was noted by Guiot that West's model assumes unrestricted dietary conditions, whereas real life tumors are rarely in such conditions. In light of this, slight disagreements with the model are acceptable, however experimental data for the growth of tumors in an unrestricted dietary environment would help significantly by removing a possible source of error.

7

IV. Conclusion

We have looked at the application of two general methods of phase transitions to the study of cancerous tumors. The first method was a local interaction model that simulated the growth of a tumor by keeping track on local interactions between cancerous and healthy cells as well as the balance of nutrients. Based on the level of nutrients in a given cell, the model gave rise to cell replication, death, or migration. The combined effect of these local processes was to generate macroscopic tumors that exhibit many of the properties seen in real tumors. These include four major tumor phases, uncontrolled growth, metastasis, latency, and regression as well as transitions between the phases. In it's initial form the model was only capable of simulating uniform soft tissue environments, however with a straightforward extension, we saw that the same model is able to describe tumor growth in far more complex environments including tumor growth in the presence of bones, cartilage, muscle, and more. Using the capabilities of the augmented model we saw simulations of tumor growth both in the larynx and near the jaw bone. Both these simulations agreed qualitatively very well with clinical observations of the same cancers, including both shape and size of the tumor. Despite these exciting developments, this model and ones similar to it are a far ways off from being everyday tools in the battle against cancer. Much more quantitative data is needed to compare the models against. Unfortunately, because cancer typically takes many years to develop and when developed is often times extremely hard to observe without invasive and very dangerous operations, good quantitative data is hard to come by.

The second method we looked at was the use of a universal scaling law to extract features that are common to a very large class of life forms. As was shown by West et al., their scaling law worked for many animals from fish to birds to mammals; from animals that have a mass on the order of a tenth of a gram to those that have a mass on the order of hundreds of kilograms. This scaling is incredible all in it's own but what is even more amazing is that this same kind of scaling applies to cancerous tumors as shown by Guiot et al.. This is perhaps due to the fact that the same laws of supply and demand apply for a rapidly growing tumor as do for a growing organism.

Understanding and perhaps one day being able to manage or cure cancer is a very challenging goal. Progress has been made on many fronts but there is still much more to do. As more and more physicists become aware of the potential of physics techniques in the biological sciences, there will surely be more attention paid to the type of problems we looked at in this paper. Perhaps one day the research tools we use today will be a part of every day clinical procedures in order to diagnose, treat and manage cancer.
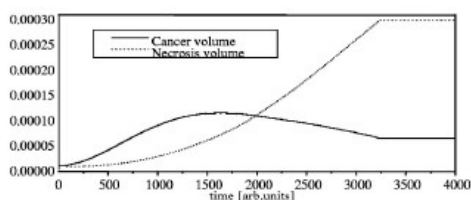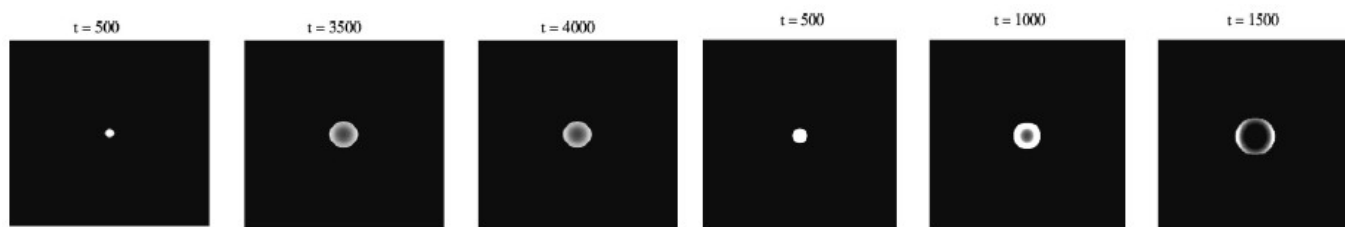
Appendix 1

Evolution of tumors for fixed γ^{as} and varying p_o. All figures are from reference 3, Delsanto et al. (2000).
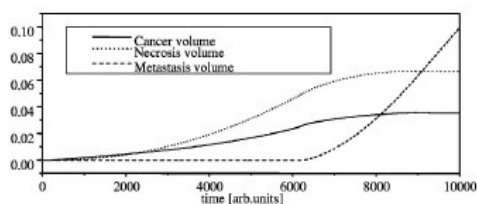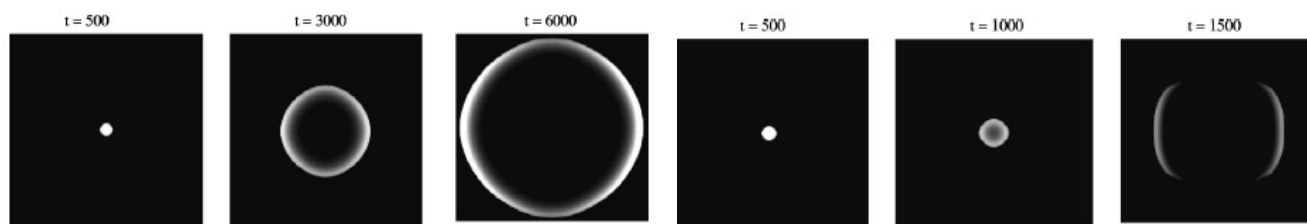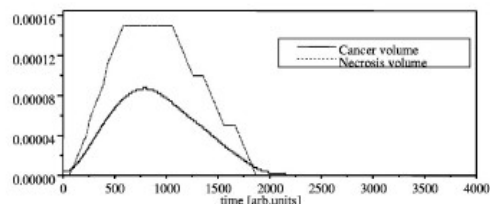

$p_o = 0.2$. *Results in unrestricted growth.*
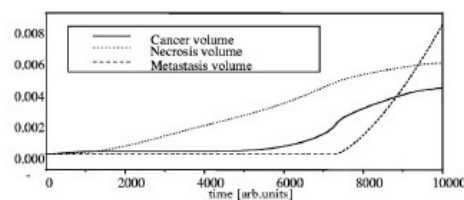
$p_o = 0.1$. *Most likely leads to metastasis.*

$p_o = 0.075$. *Resluts in latency.*

$p_o = 0.05$. *Results in regression.*

Appendix 2

Here we show various tumor data rescaled and plotted. The rescaled graphs agree very well with West's predictions for a universal growth law. All figures and tables are from reference 5, Guiot et al. (2000).
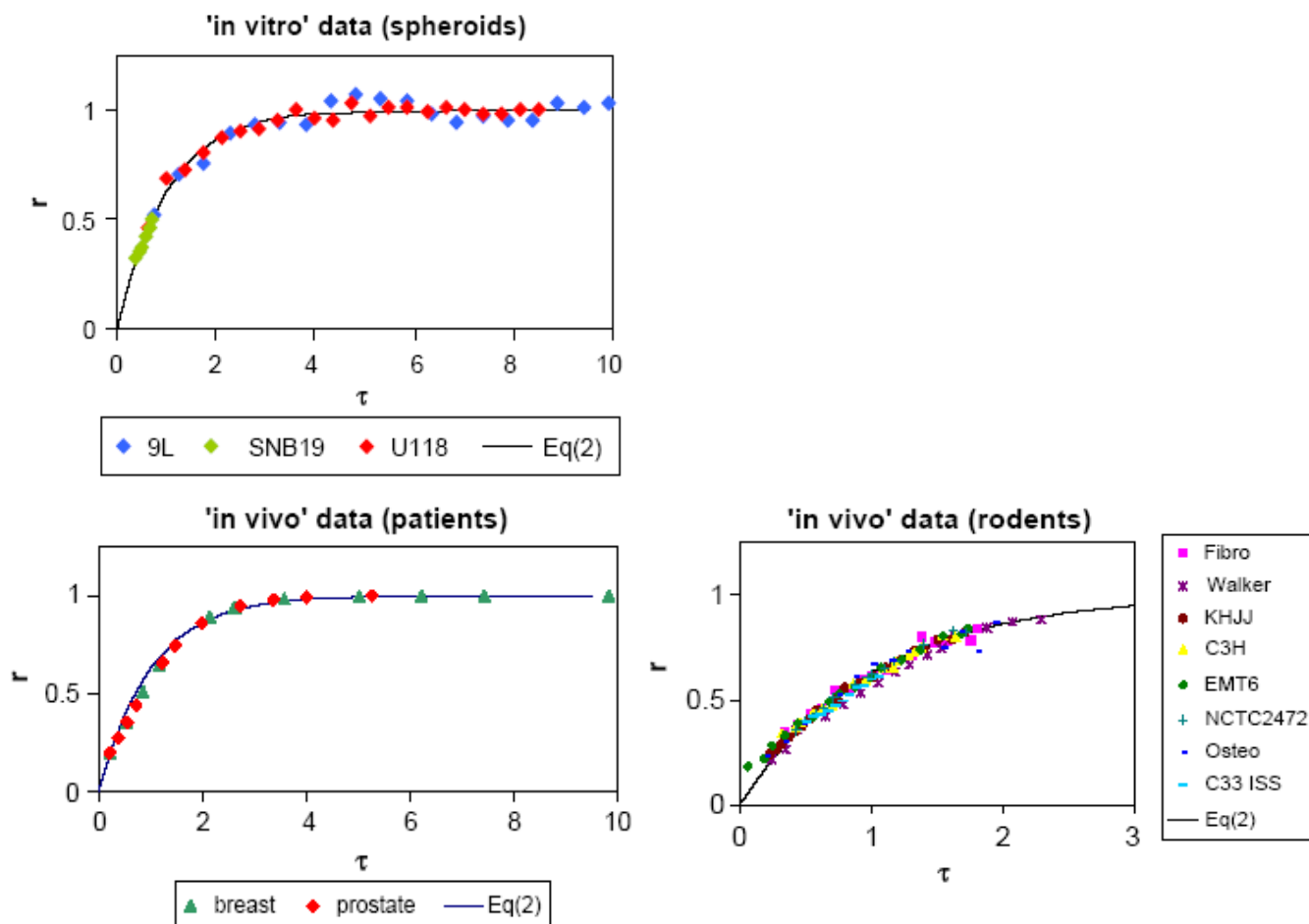

'in vitro' data (spheroids)

9L ◆ SNB19 ◆ U118 — Eq(2)

'in vivo' data (patients)

▲ breast ◆ prostate — Eq(2)

'in vivo' data (rodents)

■ Fibro
✕ Walker
● KHJJ
▲ C3H
● EMT6
+ NCTC2472
· Osteo
– C33 ISS
— Eq(2)

Table 1
Estimates of the relevant parameters from Figs. 1–3

Tumor	Reference	m_o (g)	M (g)	a ($g^{0.25}$/day)	R^2
9L	Chignola et al. (2000)	0.000037	0.000515	0.102	0.69
U118	Chignola et al. (2000)	0.000037	0.000812	0.084	0.64
SNB19	Nirmala et al. (2001)	0.025	3	0.075	0.96
Fibro	Steel (1977)[a]	1	200	0.14	0.95
Walker	Steel (1977)[a]	0.348	150	1.54	0.97
KHJJ	Steel (1977)[a]	0.0012	2	0.23	0.99
C3H	Steel (1977)[a]	0.0348	5	0.21	0.98
EMT6	Steel (1977)[a]	0.00135	3	0.5	0.99
NCTC 2472	Steel (1977)[a]	0.052	7	0.49	0.99
Osteo	Steel (1977)[a]	0.0058	7	0.124	0.92
C3H ISS	Cividalli et al. (2002)[a]	0.2	8	0.37	0.95
Human breast	Norton (1988)[a]	1	646	0.81	0.97
Human prostate	Yorke et al. (1993)[a]	1	641	0.42	0.85

The values of the parameters m_0, M and a are estimated by means of the fitting procedure described after Eq. (3). R^2 represents the correlation coefficient between actual and fitted data.
[a] Denotes in vivo data.

1 *A Survey of Models for Tumor-Immune System Dynamics,* edited by J. A. Adam and N. Bellomo (Birkhäuser, Boston, 1997)

2 M. Scalerandi, A. Romano, G. P. Pescarmona, P. P. Delsanto, and C. A. Condat, Phys. Rev. E **59**, 2206 (1999).

3 P.P. Delsanto, A. Romano, M. Scalerandi, and G.P. Pescarmona, Phys. Rev. E **62**, 2547 (2000).

4 B. Capogrosso Sansone, P. P. Delsanto, M. Magnano, and M. Scalerandi, Phys. Rev. E **64**, 021903 (2001).

5 C. Guiot, P. G. Degiorgis, P. P. Delsanto, P. Gabriele, and T. S. Deisboeck, J. Theor. Biol. **225**,147 (2003).

6 Delsanto P.P., Guiot C., Degiorgis P.G., Condat C.A., Mansury Y., Deisboeck T.S., Appl Phys Lett **85**:4225–7 (2004).

7 Deisboeck T.S., Mansury Y., Guiot C., Degiorgis P.G., Delsanto P.P., Medical Hypotheses **65**, 785-790 (2005).

8 West G.B., Brown J.H., Enquist B.J., Nature **413**:628–31 (2001).

9 P. S. Dodds, D. H. Rothman, and J. S. Weitz, J. Theor. Biol. **209**, 9 (2001).

10 Chignola, R., et al., Cell Prolif. **33**, 219-229(2000)

11 Nirmala, C., Rao, J.S., Ruifrok, A.C., Langford, L.A., Obeyesekere, M., Int. J. Oncol. **19**, 1109-1115. (2001)

12 *Growth Kinetics of Tumors,* Steel, G.G. (Clarendon Press, Oxford, 1977)

13 Cividalli, A., et al., Int. J. Radiat. Oncol. Biol. Phys. **52**, 1092-1098. (2002)

14 Norton, L., Cancer Res. **48**, 7067-7071. (1988)

15 Yorke, E.D., Fuks, Z., Norton, L., Whitmore, W., Ling, C.C., Cancer Res. **53**, 2987-2993. (1993)